

PREDICTION OF ANTEROPOSTERIOR SKELETAL RELATIONSHIPS OF THE SKULL BASE PARAMETERS USING CONE BEAM CT: A CROSS SECTIONAL STUDY

Nora Aly Al Abbady*^{ID}, Nouran Fouad Seifeldin**^{ID},
Ghada Borhan About Hussein*^{ID} and MennatAllah Hassan Attia***^{ID}

ABSTRACT

Background: Facial growth and development is crucial in orthodontic and forensic dentistry. Relating skull base parameters as foramen magnum (FM) size and shape to skeletal growth provides important indicators for craniofacial development. The study aimed to determine if there is a relation between the shape and dimensions of FM and anteroposterior (AP) skeletal relationship, and to predict skeletal class based on FM dimensions and shape.

Methods: One hundred and eleven CBCT scans were analyzed using Anatomage software assessing various skull parameters and FM shape and dimensions. All the measurements were evaluated in relation to AP skeletal relationship. Logistic regression (LR) analysis was performed to differentiate between class I and class II.

Results: The oval shape is the most frequent FM shape across all classes, whereas the rounded and irregular shapes were common in Class III. Although the shape and dimensions of FM along with other cranial dimensions showed no significant correlation with skeletal classes, mandibular length, ramus height, and gonial angle were larger in class III. The FM index in the sample was of the narrow type (<82) with the highest rate in Class I (%40.3) and mean FM index of 79.09 $8.83 \pm$. The LR model produced a modest overall correct classification of %73.33) %67.44 for class I, %60.98 for class II). The area under ROC curves of the model was equal to 0.751 which is considered acceptable.

Conclusion: The study revealed no significant differences between the shape and dimensions of FM and AP skeletal relationship and skull parameters.

KEYWORDS: Foramen Magnum, CBCT, Forensic, Anteroposterior Skeletal Relations.

* Lecturer, Oral and Maxillofacial Radiology Department, Faculty of Dentistry, Cairo University.

** Lecturer, Orthodontics Department, Faculty of Dentistry, Cairo University.

*** Assistant Professor, Forensic Medicine and Clinical Toxicology, Faculty Of Medicine, Alexandria University, Egypt.

INTRODUCTION

Forensic medicine is a multidisciplinary branch that has long been used in the medical field for the identification of unknown deceased, as well as for age estimation, sex determination and skull reconstruction^[1,2]. Bone structures are particularly valuable in forensic identification due to their high resistance to chemicals, high temperature and decomposition^[3].

Measurements for calvarium bones, including the frontal, parietal, and occipital bones, located in the cranial base are employed during forensic examination of unknown deceased to uncover their identity and personal background^[4,5]. In certain cases, as mass disasters, unrecognizable remains, or when other identification traditional methods like fingerprints, DNA or soft tissue analysis are not possible, forensic medicine may be replaced by forensic odontology depending on teeth and maxillofacial bony structures^[6,7,8].

From an orthodontic perspective, diagnosis and treatment planning starts by thoroughly understanding facial growth and development. This comprehensive knowledge helps orthodontists to address potential issues and develop more effective treatment plans and hence better treatment outcomes^[9,10,11,12]. The cranial base is a key part of the skull, that strongly affects the positioning of both maxilla and mandible. It is formed of anterior and posterior parts; the maxilla anteriorly is attached directly to the anterior part through growth sutures, while the mandible is attached indirectly to the posterior part through the temporomandibular joint. Hence, the cranial base degree of growth affects the anteroposterior (AP) skeletal development and jaw relation^[13,14,15,16].

The foramen magnum (FM), is mainly formed by the occipital bone, and is located in the cranial base at its posterior part. It is recognized as the most prominent structure of this bone due to its large

size^[17,18] yet its shape and size may vary among species and individuals^[17]. Owing to its prominent location, an association between its morphology and AP skeletal relationships could be expected. Consequently, FM morphology could serve as a valuable reference for both anatomists in forensic investigation and for orthodontists as well.

Cone beam computed tomography (CBCT) is a three dimensional (3D) maxillofacial imaging modality that helps many dental fields such as orthodontics, implantology, surgery^[19,20,21] as well as forensic dentistry^[4,22], due to its enhanced image quality, low dose, low cost, and enhanced 3D images in multiple planes. These advantages would in turn improve dental and surgical treatment planning, raising overall treatment outcomes^[4,23,24,25].

Although the correlation between the AP skeletal relationship and the cranial base measurements has been previously reported in the literature, the FM and AP skeletal relationships has never been assessed, hence, the present study's aim was three folds; to explore, for the first time, the distribution of FM various shapes in the three skeletal classes, second, to compare skull parameters with different skeletal classes and FM shape and dimensions and third, to predict the underlying AP skeletal classification using logistic regression (LR) models.

MATERIALS AND METHODS

A retrospective cross-sectional study was performed on craniofacial CBCT scans from 111 adult patients (29 males and 82 females), sourced from the database of the Oral and Maxillofacial Radiology Department, and with ages range of 18-40 years. The study was approved by the faculty of Dentistry, Cairo university ethics committee, with code number 331122.

Inclusion criteria: Craniofacial adult CBCT scans with complete FM and sound craniofacial features.

Exclusion criteria: Patients under 18 years who have history of orthodontic treatment, skeletal craniofacial disease, oral and maxillofacial trauma or surgery, or conditions that could damage the FM especially when associated with congenital syndromes.

CBCT imaging parameters

Patients were imaged using 3D CBCT machine (Planmeca Promax 3D mid, Helsinki, Finland) with 0.4 mm voxel size, and field of view of 20x20 cm, the kilovoltage and milliamperere were set at 90 kVp and 10 mA respectively for 13.891 sec.

All the CBCT DICOM images were exported and viewed on Anatomage software version 5.3. CBCT volumetric images of all subjects were initially reoriented such that the mid sagittal plane was at a right angle to the floor, ensuring precise measurements. Facial landmarks were then identified and adjusted in each case in the 3 planes (axial, sagittal, and coronal) by an expert radiologist of more than 15 years' experience (Fig. 1) generating linear and angular orthodontic measurements automatically.

Linear and angular measurements

The study generated different linear and angular orthodontic measurements and indices, which are measured following these definitions (Fig. 2 and 3).

Linear measurements were conducted including:

Sella length (SL): the distance between the tuberculum sellae and dorsum sellae.

Sella width (SW): the perpendicular line drawn from the SL to the deepest point in the sella floor.

Foramen Magnum (FM) length: the distance between the FM posterior margin midpoint (opisthion) and the FM most anterior part midpoint (bastion).

Foramen Magnum (FM) width: the distance between the FM most lateral points.

Facial height: the distance between the midpoint of both eyebrows (Glabella), to the chin lowest point.

Inter-condylar distance: the distance between the highest point of right and left condyles.

Chin length: the distance from the point in the alveolar process between the lower incisors to the midpoint of lower border of mandibular body.

Ramus height: the distance from the highest point of right condyle to a point on the external contour of the gonial angle.

Mandibular length: the distance between the previous point of the gonial angle and the chin lowest point.

Angular measurements were conducted including

SNA: Angle generated by intersection of the sella/nasion plane with nasion/A plane. It represents the AP maxillary relationship with the cranial base.

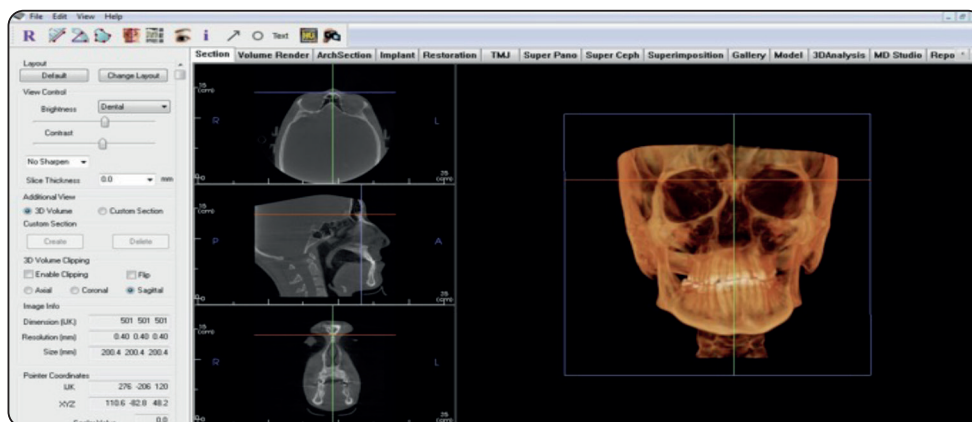


Fig. (1). Example of landmark identification and adjustment for Nasion point in axial, sagittal and coronal planes.

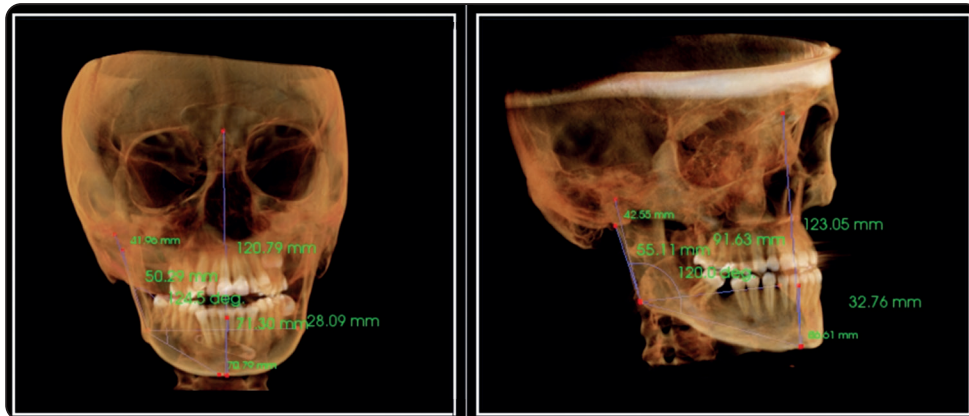


Fig. (2). Linear and angular measurements generation.

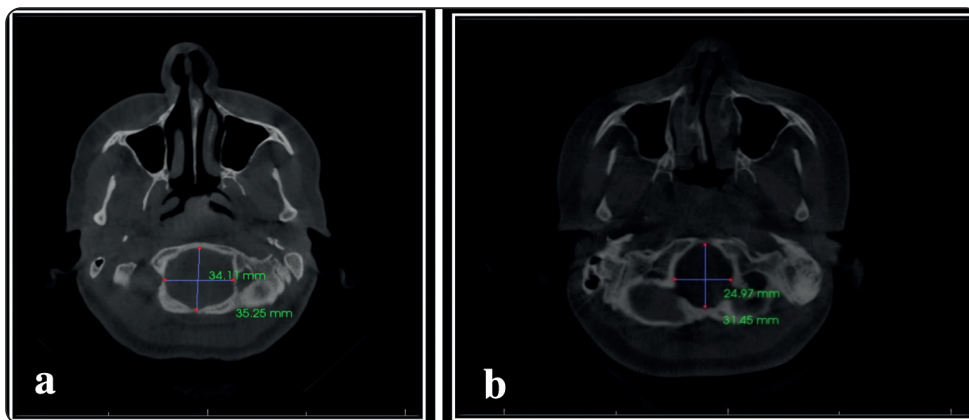


Fig. (3). Measurements of the foramen magnum's length and width, shown in a) round and b) oval shapes.

SNB: Angle generated by intersection of the sella/nasion plane and nasion/B plane. It represents the AP mandibular relationship with the cranial base.

ANB: Angle generated by intersection of the Nasion/A line and the Nasion/B line. It determines the AP skeletal relationship of the maxilla to the mandible (Skeletal classification)

Gonial angle: Angle generated between the ramus and the mandibular body.

Determination of the skeletal class using angular measurements

Steiner method (ANB angle) was used to ensure that the subjects confirmed to certain skeletal group [26]:

Group 1: ANB angle ranging from 1° to 4° , reflects skeletal class I malocclusion.

Group 2: ANB angle greater than 4° , reflects skeletal class II malocclusion.

Group 3: ANB angle less than or equal 0, reflects skeletal class III malocclusion.

Evaluation of foramen magnum

In an axial cut, a clear image of the FM was chosen to identify its shape. Visual examination of the shape of each FM was conducted and one shape was selected from the following's classification: oval, rounded, egg, tetragonal, pentagonal, hexagonal and irregular.

Using Martin and Saller classification [27] the FM index was assessed according to this formula:

$$\text{FM Width/FM Length} \times 100$$

- (a) Narrow: FM index of less than or equal to 81.9
- (b) Medium: FM index ranging from 82.0 to 85.9
- (c) Large: FM index of greater than or equal 86.0.

Intra-observer reliability evaluation

All the measurements were performed by an oral radiologist with more than 15 years' experience. The measurements were repeated two weeks later, and the average was calculated and recorded.

Statistical analysis:

Statistical analysis was performed using SPSS 20®1, Graph Pad Prism®2 and Microsoft Excel 20163. Data was represented as mean and standard deviation for quantitative data, and as frequency and percentages or qualitative data. Qualitative data were explored for normality by using Shapiro Wilk and Kolmogorov-Smirnov normality test which revealed that all data is parametric data (P-value >0.05). Accordingly, comparison between more than 2 groups was performed by One Way ANOVA followed by Tukey's Post hoc test for multiple comparisons. In qualitative data, comparisons were performed by using Fisher's exact Test. LR model was used to analyze the relationship between the classes and the a combination of various predictors from the base of skull and the mandible. LR was used to assess variables individually and in combination. Receiver operating characteristic (ROC) curve, a well-accepted test measure of predictive accuracy^[29], was used to assess the LR models.

Sample size calculation

Owing to the complex nature of our study two sample sizes were calculated according to the nature of the variables observed. For the foramen magnum shape, the sample size was calculated based on a previous study^[5]. According to this study, the minimal accepted sample size is 58 when the coefficient of determination P2 is 0.16 ($r=0.472$) between APD and TD), the effect size is 0.4, with probability (power) 0.8 and the Type I error probability associated

with this test is 0.05. Total sample size increased to 70 to compensate for 20% drop out. For the metric data, the sample size was calculated based on a previous study^[29]. The facial height was selected as a reference for the metric data. The minimal accepted sample size is 66 when the coefficient of determination P2 is 0.17, ($r=0.472$), the effect size is 0.28, with probability (power) 0.8 and the Type I error probability associated with this test is 0.05. Total sample size increased to 80 to compensate for 20% drop out. The test – correlation Point biserial model was performed by using G.Power 3.1.9.7.

RESULTS

Association between gender and foramen magnum shape:

Table 1 and figure 4 depict the frequency observed in the overall sample and the association between gender and FM shape. The most frequent FM shapes were the oval, rounded, and irregular shapes regardless of sex. For males, the oval (37.9%) and Irregular (20.7%) whereas for females the rounded (26.8%) and Oval (22.0%), Figure 5. The least common shape was Tetragonal being 3.4% for males and 4.9% for females. No statistically significant association was found between gender and FM shape ($p=0.24$).

Association between foramen magnum shapes and skeletal classes

Table 2 and figure 5 present the distribution of FM shapes across the skeletal classes I, II, and III. No statistically significant association was found between FM shape and skeletal class ($p=0.53$). The oval shape is the most common across all classes, particularly in class I and II (22.2% and 31.7%, respectively). The rounded shape is also prevalent in all classes, with the highest percentage in class III (28%). The least common shapes include tetragonal shape whereas the pentagonal, and hexagonal were most commonly found in class I. The irregular FM shape was observed more frequently in class III.

TABLE (1) The distribution of FM shapes in the overall sample and association between gender and FM shape:

	(29=Male (n		(82=Female (n		Overall		P value
	Count	%	Count	%	Count	%	
Rounded	2	%6.9	22	%26.8	24	%21.6	0.24
Oval	11	%37.9	18	%22.0	29	%26.1	
Egg	3	%10.3	9	%11.0	12	%10.8	
Tetragonal	1	%3.4	4	%4.9	5	%4.5	
Pentagonal	4	%13.8	9	%11.0	13	%11.7	
Hexagonal	2	%6.9	10	%12.2	12	%10.8	
Irregular	6	%20.7	10	%12.2	16	%14.4	

TABLE (2) Frequency and distribution of different FM shapes among each skeletal class, comparison between them using Chi square test:

FM shape	Skeletal classes						Fisher's exact Test
	(Class I (normal		(Class II (protruded		(Class III (retracted		
	Count	% Column N	Count	% Column N	Count	% Column N	
Rounded	8	%17.8	9	%22.0	7	%28.0	0.53
Oval	10	%22.2	13	%31.7	6	%24.0	
Egg	4	%8.9	6	%14.6	2	%8.0	
Tetragonal	3	%6.7	0	%0.0	2	%8.0	
Pentagonal	7	%15.6	4	%9.8	2	%8.0	
Hexagonal	8	%17.8	3	%7.3	1	%4.0	
Irregular	5	%11.1	6	%14.6	5	%20.0	

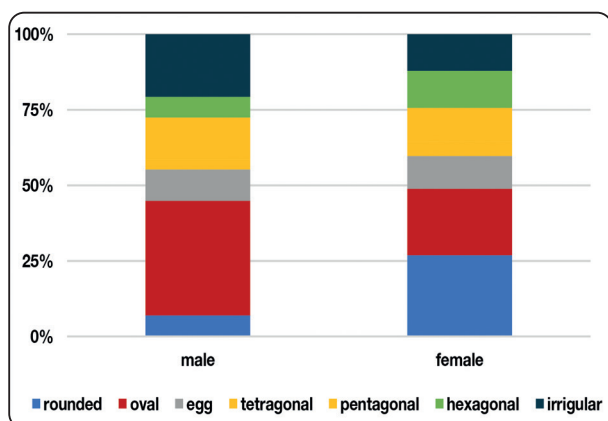


Fig. (4) Stacked bar chart representing association between gender and foramen magnum shape.

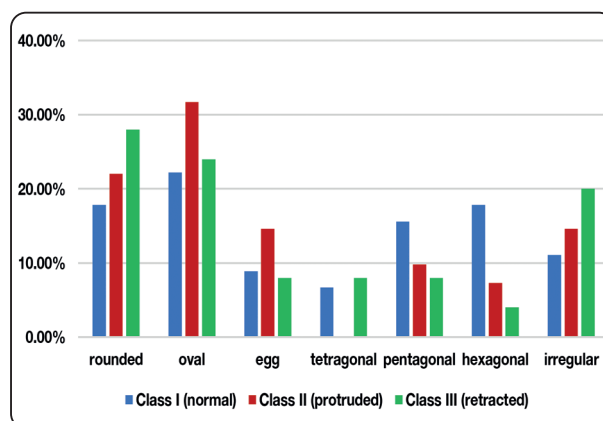


Fig. (5) Bar chart showing distribution of different foramen magnum shapes among each skeletal class.

Different parameters among skeletal classes:

Table 3 shows that the sella and FM widths and lengths were not statistically significant among the skeletal classes (P=0.05). Class III displayed the highest FM dimensions, facial height, and mandibular dimensions with the exception of intercondylar distance and chin length. Among the three skeletal classes there were no statistically significant differences regarding different measurements as the p-values were greater than 0.05 for all measurements. As expected, class II individuals had a significantly higher mean SNA angle ($87.35^{\circ} \pm 5.51$) in comparison to class I ($83.67^{\circ} \pm 3.81$) and class III ($81.28^{\circ} \pm 6.18$) as $P=0.0001$, and SNB Angle: Class III individuals had a significantly higher mean SNB angle ($85.87^{\circ} \pm 6.72$) when compared to class I ($81.29^{\circ} \pm 3.97$) and class II ($79.65^{\circ} \pm 5.08$) with $P=0.0001$.

Different parameters among different shapes of foramen magnum shape

Table 4 presents an analysis of various craniofacial measurements across different shapes of the FM. There was insignificant difference between all shapes regarding all measurements as $P>0.05$, except for the FM length and intercondylar distance. FM length, there were statistically significant differences in all shapes ($p=0.0001$). The tetragonal shape (40.5 ± 3.89) and egg shape (40.47 ± 4.32), and oval shape (41.18 ± 3.62) have significantly longer FM lengths compared to rounded (35.86 ± 3.79) and irregular shapes (35.85 ± 6.02). Intercondylar distance showed significant differences were observed ($p=0.02$). Oval shape had the largest FM dimensions, mandibular length (82.61 ± 5.67) intercondylar distance (96.95 ± 4.73). The tetragonal shape had the smallest sella length (8.78 ± 1.94) chin length (31.65 ± 5.35), ramus height (49.42 ± 4.56), and facial height (115.17 ± 9.07).

TABLE (3) Mean and standard deviation of all parameters among skeletal classes, comparison between different classes:

	Skeletal class						P value
	Class I (normal)		Class II (protruded)		Class III (retracted)		
	Mean	Standard Deviation	Mean	Standard Deviation	Mean	Standard Deviation	
Age	a 22.73	4.91	a 22.44	5.10	a 21.60	3.20	0.681
(Sella width (SW	a 8.03	1.08	a 8.25	1.22	a 8.01	1.48	0.647
(Sella length (SL	a 9.54	1.74	a 10.00	1.59	a 10.13	1.72	0.285
FM length	a 37.98	4.14	a 38.45	4.52	a 38.71	5.39	0.796
FM width	a 29.85	3.27	a 29.44	2.82	a 30.40	2.96	0.464
Inter-condylar distance	a 94.13	5.64	a 95.72	5.12	a 94.23	4.70	0.324
Chin length	a 32.32	3.50	a 33.34	3.61	a 32.58	2.95	0.372
Ramus height	a 53.30	4.25	a 53.75	5.56	a 55.40	6.66	0.282
Mandibular length	a 80.76	5.78	a 80.04	4.38	a 81.58	6.29	0.535
Gonial angle	a 125.81	6.07	a 123.05	7.20	a 126.21	10.48	0.158
SNA angle	a 83.67	3.81	b 87.35	5.51	a 81.28	6.18	*0.0001
SNB angle	a 81.29	3.97	a 79.65	5.08	b 85.87	6.72	*0.0001
Facial height	a 120.49	7.50	a 119.48	8.00	a 120.77	8.35	0.769

*Significant difference as $P<0.05$.

Means with different superscript letters were significantly different as $P<0.05$.

Means with the same superscript letters were insignificantly different as $P>0.05$.

TABLE (4) Mean and standard deviation of all parameters among different shapes of FM shape, comparison between different classes Independent t test:

	FM shape														P value
	Rounded		oval		Egg		tetragonal		pentagonal		hexagonal		irregular		
	M	SD	M	SD	M	SD	M	SD	M	SD	M	SD	M	SD	
Age	22.38	4.24	22.25	5.61	21.55	3.50	22.75	4.27	23.33	3.70	22.40	4.74	22.38	5.65	0.99
(Sella width (SW	8.51	1.38	7.65	1.13	7.73	1.14	8.04	73.	8.35	1.50	8.04	1.19	8.51	87.	0.11
(Sella length (SL	9.62	1.32	9.67	1.35	9.12	1.65	8.78	1.94	10.79	2.28	9.93	1.89	10.54	1.67	0.06
FM length	a 35.86	3.79	b 41.18	3.62	b 40.47	4.32	b 40.50	3.89	ab 37.72	3.25	ab 37.20	2.46	a 35.85	6.02	*0.0001
FM width	30.12	3.11	30.43	3.84	28.83	2.29	30.16	1.71	29.27	2.71	29.13	2.72	29.87	2.61	0.71
Inter-condylar distance	93.92 ab	5.71	a 96.95	4.73	95.29 ab	3.39	92.10 ab	2.26	ab 93.87	6.70	b 90.94	3.99	95.93 ab	5.19	*0.02
Chin length	31.86	3.82	32.92	3.41	34.01	2.86	31.65	5.35	33.69	3.48	31.80	3.20	33.15	2.56	0.43
Ramus height	52.80	3.57	54.25	6.55	55.43	6.09	49.42	4.56	55.47	4.14	52.88	5.29	54.91	5.46	0.26
Mandibular length	78.46	6.07	82.61	5.67	79.37	3.35	81.18	5.97	81.26	3.57	79.44	5.09	81.80	5.66	0.12
Gonial angle	124.29	9.17	125.04	7.80	125.13	7.27	126.48	8.63	125.40	4.59	124.67	7.45	124.54	8.73	0.99
SNA angle	83.93	4.62	85.39	5.34	85.53	7.33	83.34	4.06	85.47	3.69	84.61	7.09	82.41	6.31	0.65
SNB angle	81.61	6.24	81.82	5.55	81.50	4.94	82.66	4.38	82.96	4.01	80.51	5.53	81.42	7.04	0.12
Facial height	116.86	8.78	121.88	7.86	122.12	5.95	115.17	9.07	120.82	6.01	119.39	8.73	122.26	6.57	0.12

*Significant difference as $P < 0.05$; Means with different superscript letters were significantly different as $P < 0.05$; Means with the same superscript letters were insignificantly different as $P > 0.05$.

Distribution foramen magnum size indices among each skeletal class

Table 5 presents the distribution and measurements of FM size indices across three skeletal classes: Class I, II, and III. The mean values of the overall sample in each class showed the FM index was of the narrow type (<82) according to Martin and Saller classification. The mean FM index in class I, II, III was 79.09 ± 8.83 , 77.40 ± 10.18 , 79.28 ± 7.98 , correspondingly. Males FM index (85.01 ± 8.67) was higher than females index (83.17 ± 7.78), with no statistically significant ($P > 0.05$). The study revealed that narrow FM was the most common across all classes where the highest percentage was in class I (40.3%). The comparison of mean values across classes I, II, and III were 74.20, 71.28, and

74.60, respectively showed a marginal statistical significance ($p = 0.06$). In contrast, large FM was the least common overall. The highest prevalence in class II (50%). Widest range of mean values (91.30 - 95.11). Overall, no statistically significant differences were found in FM size distribution across the skeletal classes $P > 0.05$.

Logistic regression for prediction of the skeletal class

In this study, a LR model was developed to determine the craniofacial metric variables responsible for the discrimination of skeletal class I and II. The equations established by LR is summarized in Table 6. The multivariate forward stepwise regression approach detected integrated four variables (sex, sella length, intercondylar distance, and FM

width). Although the FM width was insignificant, it affected the overall accuracy of the model when removed. This equation provided a modest overall correct classification of 67.44% (73.33% for class

I, 60.98% for class II) as displayed in Table 7. The model diagnostic analysis by the area under ROC curves (AUC) of the LRA model was equal to 0.751 which is considered acceptable (Figure 6).

TABLE (5) Frequency, distribution, mean and standard deviation of different FM size indices among each skeletal class:

Foramen magnum index	Skeletal class												One Way ANOVA test P value
	Class I (normal)				Class II (protruded)				Class III (retracted)				
	N	%	Mean	SD	N	%	Mean	SD	N	%	Mean	SD	
Narrow	29	%40.3	74.20	5.25	27	%37.5	71.28	5.85	16	%22.2	74.60	3.73	0.06
Medium	10	%52.6	83.69	0.98	4	%21.1	83.95	1.57	5	%26.3	83.44	1.54	0.18
Large	6	%30.0	95.11	6.43	10	%50.0	91.30	3.77	4	%20.0	92.84	6.80	0.97
Overall	45	%40.3	79.09	8.83	41	%37.5	77.40	10.18	25	%22.2	79.28	7.98	0.62

TABLE (6) Logistic regression model and estimated odds ratios with confidence intervals

	Coefficient B	Standard error	z	p	Odds Ratio	conf. interval %95
Constant	14.24-	5.33	2.67	0.008	0	0.02 - 0
sex F	2.21	0.73	3.04	0.002	9.08	37.73 - 2.19
(Sella length (SL	0.34	0.16	2.14	0.033	1.41	1.92 - 1.03
FM width	0.15-	0.09	1.65	0.1	0.86	1.03 - 0.73
Inter-condylar distance	0.14	0.05	2.61	0.009	1.15	1.28 - 1.04

TABLE (7) Confusion matrix and classification rates for skeletal class I and II.

Observed	Predicted		Correct
	1 Class	2 Class	
1 Class	33	12	%73.33
2 Class	16	25	%60.98
Total			%67.44 (86/58)

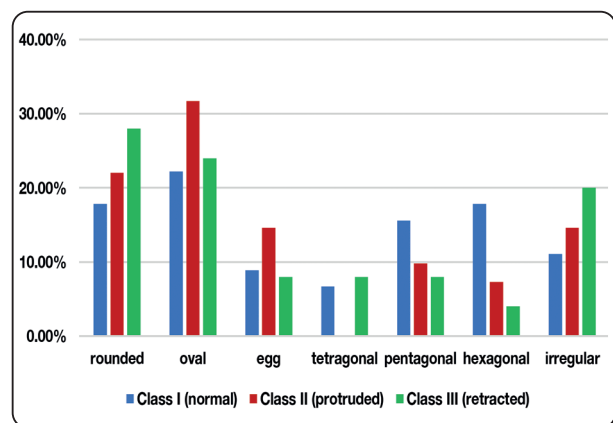


Fig. (6) The Receiver-operating characteristic (ROC) curve of the model together with the area under the curve (AUC) =0.751

DISCUSSION

The cranial base, due to its close proximity and connection to the facial bones, significantly influences the growth and development of various facial structures and impacts facial morphology^[16]. It extends anteriorly from the foramen caecum to the basioccipital bone posteriorly. The sella turcica splits the cranial base into an anterior and posterior compartment, with the anterior compartment extending to frontonasal suture, and the posterior compartments, extending to FM anterior border, known as basion. The anterior compartment articulates with the maxilla, while the posterior compartments articulate with the mandible. Thereby, any alteration in these articulations would change the position of maxilla and mandible in relation to the cranial base, affecting the skeletal pattern and the occlusion type^[13]. It has been reported^[30] that cranial base morphology varies among different skeletal patterns, with individuals exhibiting skeletal class III tend to have a smaller angle and shorter length of the cranial base^[16].

Understanding anatomical variation of FM as a part of cranial base can provide valuable insights in forensic identification and prediction, as well as aiding in the ability to diagnose craniofacial disorders. Thus, this study investigated the FM shape and size variation in relation to AP skeletal relation in Egyptian population. As recommended by Nanda^[31] patients over the age of 18 were only included in the study to ensure that most growth changes had been completed.

In agreement with other studies of various populations^[32,33,34,35,36,37], the most common shape of FM observed in our study was oval (26.1%). In contrast to this finding other studies^[38,39,40] identified the rounded shape as the most common. Our study found that while the oval is the most common, rounded shape followed it closely, accounting for 21.6% of the cases and aligning with Singh, D et al. findings^[41]. Additionally, our results concluded that oval shape was the most common across all

skeletal classes. However, the round shape was also frequently observed, and showed the highest percentage in class III.

Earlier studies^[42,43,44] revealed that skeletal classes exhibit some cephalometric variations, and reported that skeletal class III were more likely to have sella turcica bridging compared to class I and class II skeletal classes. Consistent with our findings, Chou et al.^[45] found no significant differences in sella dimensions across different skeletal classes. Furthermore, our results showed that class III exhibited the largest ramus height, mandibular length, gonial angle, and facial height dimensions despite having insignificant differences. This finding aligns with Al Maaitah et al.^[15] who reported larger mandibular body length and gonial angle in class III individuals. Other studies^[13,46,47] have also supported these findings.

The majority of studies^[33,34,36,41] have focused on measuring the foramen magnum's length and width, primarily for sex prediction. The average dimensions reported were approximately 35 mm in length and 30 mm in width,^[13] confirming that the FM is generally larger in males across different populations^[48,49,50,51]. However, these studies did not investigate the relation between FM dimensions and AP skeletal relationship. Although these dimensions varied across different skeletal classes, the differences were not statistically significant. Our findings indicate that class III skeletal relationships exhibited the largest FM dimensions, while class I had the narrowest.-

There are different prediction methods available for craniofacial growth such as averages of growth increments and the maxillary longitudinal growth^[52], the facial types^[53], and mathematical models based on cephalometric data^[54,55,56]. Buschang et al.^[54] evaluated the maxillary and mandibular growth using two variables, which are: Mandibular length (Ar-Po) and the ramus length (Ar-Go). Additionally, the mandibular ramus, angle of the skull base and

angle of the mandibular plane was employed by Baccetti et al, ^[57] to predict class III. In this study, we attempted to predict the skeletal class using a set of cranial base measurements. Despite the relatively modest accuracy obtained by the model (67.44%), the model has potentials to distinguish between class I and II using few variables namely gender, sella length, foramen magnum width, and intercondylar distance. These findings refer to the influence of the base of skull development on the skeletal class. The cranial base dimensions are essential in determining the maxillary length, the condyle positioning, and in turn, the mandible ^[58].

CONCLUSION

Our findings demonstrated that morphological evaluation of the FM shape in the Egyptian population and the skull measurements didn't differ among different anteroposterior skeletal classes. Subtle differences were detected by the LR equation indicating limited usefulness for classifying the AP skeletal relationship.

Limitations

The male-to-female ratio was low, reflecting a smaller number of males in comparison to females. The sample size was relatively small, and more cases should be added to class III in order to include it in the logistic regression analysis.

ACKNOWLEDGEMENT

Not applicable.

Author Contributions:

M.H. Conceived the idea, developed and wrote the statistical theories and methodologies. N.A. was responsible for data collection and CBCT analysis as well as manuscript writing. N.F contributed to data collection and revised the manuscript, G.B focused on manuscript revision.

Funding

No funding.

Conflict of interest

The authors state that they have no conflicts of interests.

REFERENCES

1. Christensen AM, Passalacqua NV, Bartelink EJ. Forensic Anthropology: Current Methods and Practice. Academic Press; 2014.
2. Byers SN. Introduction to Forensic Anthropology. 5th ed. New York: Routledge; 2021.
3. Gopal SK. Role of 3D cone beam computed tomography imaging in forensic dentistry: A review of literature. Indian Forensic Odontol. 2018;11:75-82.
4. Issrani R, Prabhu N, Sghaireen MG, Ganji KK, Alqahtani AMA, AlJamaan TS, et al. Cone-beam computed tomography: A new tool on the horizon for forensic dentistry. Int J Environ Res Public Health. 2022;19:5352.
5. Vinutha SP, Suresh V, Shubha R. Discriminant function analysis of foramen magnum variables in the South Indian population: A study of computerized tomographic images. Anat Res Int. 2018;2018:2056291.
6. Pretty IA, Sweet D. A look at forensic dentistry – Part 1: The role of teeth in the determination of human identity. Br Dent J. 2001;190(7):359-66.
7. Cameriere R, Ferrante L, Cingolani M. Age estimation in children by measurement of open apices in teeth. Int J Legal Med. 2004;118(2):100-3.
8. Gomez-Polo C, Martin de las Heras S. The role of the maxillofacial skeleton in forensic identification: A review of methods and techniques. J Forensic Sci. 2020;65(1):231-43.
9. Papageorgiou SN, Koletsi D, Iliadi A, Gkantidis N, Bourauel C. Clinical effectiveness of orthodontic treatment: A systematic review and meta-analysis. Eur J Orthod. 2019;41(6):605-16.
10. Alarcón JA, Bastir M, Rosas A, Ríos L. 3D analysis of craniofacial growth in relation to orthodontic diagnosis and treatment planning. J Clin Med. 2020;9(3):801.

11. Kau CH, Lee RJ. The future of orthodontics: Implications of 3D facial growth and development understanding. *Am J Orthod Dentofacial Orthop.* 2021;159(3):317-24.
12. McNamara JA, Franchi L. The role of craniofacial growth in orthodontic diagnosis and treatment planning. *Semin Orthod.* 2022;28(2):100-10.
13. Vandekar M, Kulkarni P, Vaid N. Role of cranial base morphology in determining skeletal anteroposterior relationship of the jaws. *J Ind Orthod Soc.* 2013;47(4):245-8.
14. Alhazmi N, Almihbash A, Alrusaini S, Bin Jasser S, Alghamdi MS, Alotaibi Z, et al. The association between cranial base and maxillomandibular sagittal and transverse relationship: A CBCT study. *Appl Sci.* 2022;12:9199.
15. Al Maaitah EF, Alomari S, Al-Khateeb SN, Abu Alhaija ES. Cranial base measurements in different anteroposterior skeletal relationships using Bjork-Jarabak analysis. *Angle Orthod.* 2022;92(5):613-8.
16. Dileep S, Khader MA, Ali H, Paul KD, Narayan M, Jayan A. Cranial base parameters in adults with skeletal class I and class II skeletal pattern. *J Orthod Sci.* 2022;11:41.
17. Demir BT, Eşme S, Patat D, Bilecenoğlu B. Clinical and anatomical importance of foramen magnum and craniocervical junction structures in the perspective of surgical approaches. *Anat Cell Biol.* 2023;56(3):342-9.
18. Celik NG, Akman B. Anatomical analysis of foramen magnum: A 3D Slicer CT study. *Med Records.* 2023;5(Suppl 1):182-6.
19. Gupta J, Ali SP, Singh S, Bhardwaj G, Bansal S, Goel N. Applications of cone beam computed tomography in dentistry. *J Family Med Prim Care.* 2020;9(8):3857-63.
20. Guncu GN, Aksakalli S. Cone-beam computed tomography in orthodontics: Current applications and future directions. *J Orthod.* 2021;48(3):239-51.
21. Liu Y, Xu Y. The impact of cone-beam computed tomography on orthodontic diagnosis and treatment outcomes: A meta-analysis. *J Dent Res.* 2023;102(4):435-43.
22. Sinha S. Role of maxillofacial radiology in expediting forensic odontology. *Int J Oral Care Res.* 2020;6(4).
23. Pauwels R, Jacobs R. The benefits of cone-beam computed tomography in dentistry: A review of recent advances. *J Dent Res.* 2021;100(5):569-75.
24. Kamburoğlu K, Pehlivanoglu E. The advantages of cone-beam computed tomography in diagnostic dentistry: A comparative study. *Clin Oral Investig.* 2022;26(1):123-31.
25. Sharma N, Gupta M. Evaluating the clinical benefits of cone-beam computed tomography in oral and maxillofacial surgery. *J Oral Maxillofac Surg.* 2023;81(6):1034-42.
26. Jacobson A, Jacobson R. Radiographic cephalometry: from basics to 3D imaging. 2nd ed. Chicago: Quintessence; 2006.
27. Govsa F, Ozer MA, Celik S, Ozmutaf NM. Three-dimensional anatomic landmarks of the foramen magnum for the craniovertebral junction. *J Craniofac Surg.* 2011;22(3):1073-6.
28. Nick TG, Campbell KM. Logistic regression. *Methods Mol Biol.* 2007;404:273-301.
29. Ide J, Rynn C. The importance of the cranial base in orthodontics: A review. *J Orthod.* 2020;47(3):228-233.
30. Sanggarnjanavanich S, Sekiya T, Nomura Y. Cranial base morphology in adults with skeletal Class III malocclusion. *Am J Orthod Dentofacial Orthop.* 2014;146:82-91.
31. Nanda SK. Growth patterns in subjects with long and short faces. *Am J Orthod Dentofacial Orthop.* 1990;98:247-58.
32. Nagwani M, Rani A, Rani A. A morphometric and comparative study of foramen magnum in North Indian population. *J Anat Soc India.* 2016;65(Suppl 1).
33. Vinutha SP, Shubha R. Morphometry and sexual dimorphism in foramen magnum: A study of human skull bones. *Int J Anat Res.* 2016;4(3):2593-9.
34. Rajkumar K, Prabhakaran K, Punita M, Vikram S. Morphometric analysis of the foramen magnum of dry human skulls in North Indian population. *Int J Anat Res.* 2017;5(1):3480-4.
35. Dasegowda G, Padmalatha K, Priyanka BP, Mirmire S. Morphology and morphometric analysis of foramen magnum in adult human skulls. *Int J Anat Res.* 2020;8(4.1):7771-6.
36. Bahşi İ, Adanır SS, Orhan M, Kervancioğlu P, Büyükbeşe ZS, Beger O, Yalçın ED. Anatomical evaluation of the foramen magnum on cone-beam computed tomography images and review of literature. *Cureus.* 2021;13(11)
37. Singh R, Verma S, Arti, Kumar V. Morphometric and morphological study of foramen magnum. *J Phys Ther Clin Pract.* 2024;31(6):1685-9.
38. Chethan P, Prakash KG, Murlimanju BV. Morphological analysis and morphometry of the foramen magnum: an anatomical investigation. *Turk Neurosurg.* 2012;22(4):416-9.

39. Natsis K, Piagkou M, Skotsimara G. A morphometric anatomical and comparative study of the foramen magnum region in a Greek population. *Surg Radiol Anat.* 2013;925-34.
40. Degno S, Abrha M, Asmare Y, Muche A. Anatomical variation in morphometry and morphology of the foramen magnum and occipital condyle in dried adult skulls. *J Craniofac Surg.* 2019;30(1):256-9.
41. Singh D, Patnaik P, Gupta N. Morphology and morphometric analysis of the foramen magnum in dried adult skulls in the North Indian region. *Int J Health Sci Res.* 2019;9(4):36-42.
42. Leonardi R, Barbato E, Vichi M. Sella turcica bridging and morphology in skeletal Class III patients: A cephalometric study. *J Clin Orthod.* 2018;52(2):97-104.
43. Alkofide EA, Alnamankani E. Sella turcica morphology and bridging in different skeletal patterns: A retrospective cephalometric study. *Orthod Craniofac Res.* 2017;20(1):37-45.
44. Sathyanarayana HP, Naik VB, Suresh S. Sella turcica bridging in patients with skeletal Class III malocclusion: A comparative study. *Am J Orthod Dentofacial Orthop.* 2019;156(3):352-9.
45. Chou ST, Chen CM, Chen PH, Chen YK, Chen SC, Tseng YC. Morphology of sella turcica and bridging prevalence correlated with sex and craniofacial skeletal pattern in Eastern Asia population: CBCT study. *Biomed Res Int.* 2021;6646406.
46. Gasgoos SS, Al-Saleem NR, Awni KM. Cephalometric features of skeletal Class I, II and III: A comparative study. *Al-Rafidain Dent J.* 2007;7:122-30.
47. Proff P, Will F, Bokan I, Fanghänel J, Gedrange T. Cranial base features in skeletal Class III patients. *Angle Orthod.* 2008;78:433-9.
48. Abbas A, Saleh R. Sexual dimorphism of foramen magnum: an Egyptian study. *Egypt J Forensic Sci.* 2023;13(1):14.
49. Raguz M, Hrabac P, Sedmak D, Gjurasin M, Kovacic N. Diameters and bone thickness at the margin of the foramen magnum in dry skulls from pediatric population: a cross-sectional anatomical study. *Childs Nerv Syst.* 2017;33(5):819-23.
50. Sharma N, Sharma RK. Morphometric study of the foramen magnum in adult Indian human skulls. *J Clin Diagn Res.* 2022;16(5).
51. Kumar R, Nagarajan K. Sexual dimorphism in cranial base dimensions with specific reference to foramen magnum: a CT study. *J Forensic Radiol Imaging.* 2023;5(3):115-20.
52. Solow B, Siersbaek-Nielsen S. Cervical and craniocervical posture as predictors of craniofacial growth. *Am J Orthod Dentofacial Orthop.* 1992;101:449-58.
53. Lavergne J. Morphogenetic classification of malocclusion as a basis for growth prediction and treatment planning. *Br J Orthod.* 1982;9:132-45.
54. Buschang PH, Tanguay R, Turkewicz J, Demirjian A, La Palme L. A polynomial approach to craniofacial growth: description and comparison of adolescent males with normal occlusion and those with untreated Class II malocclusion. *Am J Orthod Dentofacial Orthop.* 1986;90:437-42.
55. Arias MI, Álvarez G, Botero L, Velásquez LM. Variables cefalométricas asociadas con el desarrollo de maloclusión esquelética clase I y II. *CES Odontol.* 2006;19(2):9-16.
56. Auconi P, Scazzocchio M, Defraia E, McNamara JA, Franchi L. Forecasting craniofacial growth in individuals with Class III malocclusion by computational modelling. *Eur J Orthod.* 2014;36:207-16.
57. Baccetti T, Franchi L, McNamara JA. Cephalometric variables predicting the long-term success or failure of combined rapid maxillary expansion and facial mask therapy. *Am J Orthod Dentofacial Orthop.* 2004;126:16-22.
58. Jiménez-Silva A, Carnevali-Arellano R, Vivanco-Coke S, Tobar-Reyes J, Araya-Díaz P, Palomino-Montenegro H. Craniofacial growth predictors for Class II and III malocclusions: a systematic review. *Clin Exp Dent Res.* 2021;7:242-62.